Study of the inhibition layer formed in a ga bath on a trip mn-al steel

Andreea Paunoiu, Jean-Michel Mataigne, Florence Bertrand, David Zapico Álvarez, Jonas Staudte, Marie-Laurence Giorgi

STUDY OF THE INHIBITION LAYER FORMED IN A GA BATH ON A TRIP MN-AL STEEL

Andreea Paunoiu[1,2], Jean-Michel Mataigne[1], Florence Bertrand[1], David Zapico Álvarez[1], Jonas Staudte[1], Marie-Laurence Giorgi[2]

[1] ArcelorMittal Global R&D - Maizières Automotive Products,
Voie Romaine, 57283 Maizières-lès-Metz

[2] Laboratoire de Génie des Procédés et Matériaux (LGPM), CentraleSupélec, Université Paris-Saclay,
Grande Voie des Vignes, 92295 Châtenay-Malabry, France

ABSTRACT

The nature of the inhibition layer formed on an industrially galvanized TRIP Mn-Al substrate was investigated. The Zn bath contained low Al content (0.122 wt.%) as generally used before GalvAnnealing (GA) treatment. Prior to hot-dipping, the steel was recrystallized in a gas atmosphere with different oxygen potentials (Dew Point - *DP*), -40 and -5°C. The morphology and the nature of selective oxides at the steel surface changed from Al-Mn-O film in low *DP* annealing conditions to MnO nodules in high *DP*. In-depth characterization of the inhibition layer revealed that it is biphasic, namely $Fe_2Al_5Zn_x$ and δ, regardless the DP of annealing atmosphere. The $Fe_2Al_5Zn_x$ layer is discontinuous with δ on top. The selective oxides formed during recrystallization annealing were found to be embedded in the inhibition layer. A mechanism accounting for the formation of the inhibition layer in GA bath in presence of selective oxides is proposed in this paper. It will also be highlighted that the nature of the inhibition layer does not depend on the substrate.

Keywords: TRIP Mn-Al, selective oxides, hot-dipping, inhibition layer, GA bath

INTRODUCTION

Commonly referred to as the inhibition layer, a thin intermetallic layer is formed between the zinc overlay and the steel substrate during hot-dipping in a GA bath (Fe saturated Zn bath with 0.110-0.135 wt.% Al). Many controversial results related to the structure of this layer on IF substrates are proposed in the literature [1-7]. It has been reported that the inhibition layer was either formed as a single phase of metastable $Fe_2Al_5Zn_x$ [1,2] or as transient $FeAl_3$ [3,4] and $FeAl_2$ [4] with $Fe_2Al_5Zn_x$. Other studies revealed a biphasic structure comprised of a δ ($FeZn_7$) layer over a metastable $Fe_2Al_5Zn_x$ layer [5,6]. Nevertheless, by taking into account the Al-Fe-Zn ternary phase diagram at 460°C [7], the inhibition layer in a GA bath should contain the δ ($FeZn_7$) phase, which is in thermodynamic equilibrium with the liquid phase.

The challenge of producing lighter automotive structures with improved crashworthiness has led to the development of new steel grades such as TRansformation-Induced Plasticity (TRIP) steels containing higher concentrations of alloying elements such as Mn, Si and Al. These elements undergo oxidation during recrystallization annealing, influencing the reactivity between the substrate and the liquid Zn [8-10]. In-depth characterization of the galvanized interface in presence of selective oxides was performed in the case of GI baths (~ 0.2 wt.% Al) on steel grades such as TRIP Mn-Si [9] and Dual-Phase [11,12]. In these studies the inhibition layer consisted of $Fe_2Al_5Zn_x$ as expected for GI baths[7]. Moreover, they examined the selective oxidation state after hot-dipping showing that the oxides were incorporated into the inhibition layer. No quantitative data related to the structure of the inhibition layer formed in a GA bath on high alloyed steels is available in the literature. Hence, the main goal of this study is to investigate the nature of the inhibition layer formed in a GA bath in presence of selective oxides on a TRIP Mn-Al steel grade.

EXPERIMENTAL PROCEDURE

The substrate used in the present work was a cold-rolled *TRIP 780* MnAl steel. Its chemical composition is shown in Table 1. The analysis was performed by means of Spark-Optical Emission Spectrometry (Spark-OES) in ArcelorMittal laboratories. The steel has been industrially coated in a Fe saturated Zn bath with 0.122 wt. % Al at T = 460°C on a Continuous Galvanizing line (CGL) with the Galvannealing inductor turned off. Prior to hot-dipping, recrystallization annealing was performed at 860°C during 129 s in a N_2 + 3 vol.% H_2 gas mixture with dew point *DP* =-40 and -5°C. In parallel, the recrystallization annealing cycle was simulated using an IWATANI Rhesca device in order to evaluate the selective oxidation state of the substrate. The recrystallization annealing trials were performed at laboratory scale,

because sampling just after annealing and before hot-dipping was not possible on CGL.

Table 1: Chemical composition (wt.%) of TRIP steel investigated

C	Mn	Al	Si
0.22	1.65	1.5	0.08

The selective oxidation state of annealed samples was characterized by means of Glow-Discharge Optical Emission Spectroscopy (GDOES-Horiba Jobin Yvon GD Profiler 2) and Energy Dispersive X-ray (EDX) in a Scanning Electron Microscope (FEG-SEM, JEOL JSM-7800F). The EDX mapping was performed on cross section specimens prepared through Ar+ ion beam Cross Section Polishing (CSP - JEOL SM-09010) technique. A nickel layer was deposited after annealing treatment for the sake of EDX analysis on cross section samples.

Concerning the galvanized samples, the steel/coating interface was investigated on CSP specimens using SEM and EDX elemental mappings. In addition, Focused Ion Beam (FIB, SII Nanotechnology Inc SMI 3050TB) thin foils were prepared after selective dissolution of the Zn overlay. The FIB thin foils were analyzed by EDX and Electron Diffraction in a Transmission Electron Microscope (TEM, JEOL JEM-2100F) in order to determine the nature of the phases present in the inhibition layer.

RESULTS

1. Selective oxidation

Figure **1**(a) shows a cross-section micrograph of the steel annealed in laboratory in a low *DP* (-40°C) atmosphere. Al enrichment on the steel surface can be observed on the corresponding elemental mapping (Figure 1(b)). In addition, GDOES spectra (Figure **1** (c)) confirm the external selective oxidation of Al and Mn. Hence, it can be inferred that Al and/or Al-Mn film oxides formed on the steel surface during recrystallization annealing in a low *DP*. It should be noted that the Al signal appearing underneath the surface does not correspond always to Al-rich oxides. The rod shape of some Al-rich particles seems to correspond to AlN nitrides as analyzed by Li et al. [13].

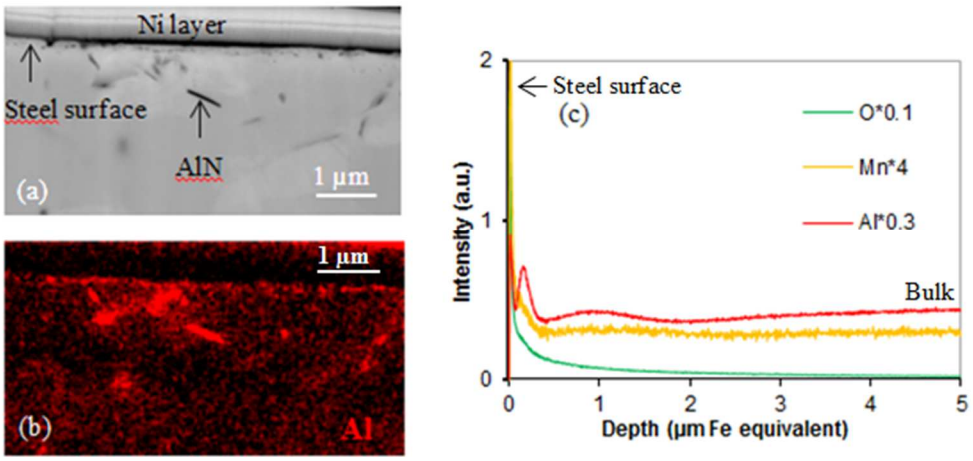

Figure 1: (a) SEM micrograph of the CSP specimen annealed in a gas atmosphere with *DP* =-40°C, (b) Qualitative elemental mapping of Al (EDX, in red) and (c) GDOES spectra of O, Mn and Al

By increasing the *DP* of the annealing atmosphere to 0°C, nodular Mn-rich oxides precipitated on the steel surface as illustrated on the EDX mapping of Mn in Figure 2 (b). Moreover, Mn oxidation occurred also within the sub-surface. Both EDX mapping and GDOES spectrum surface (Figure 2 (c and d)) clearly show that Al underwent oxidation essentially within the sub-surface and on a longer depth than Mn. The Mn-rich external oxides have been reported as MnO by Bellhouse et al. [8] and Maki et al. [14] on steel grades with comparable chemical composition in high *DP* annealing conditions (*DP* = 0, +5°C).

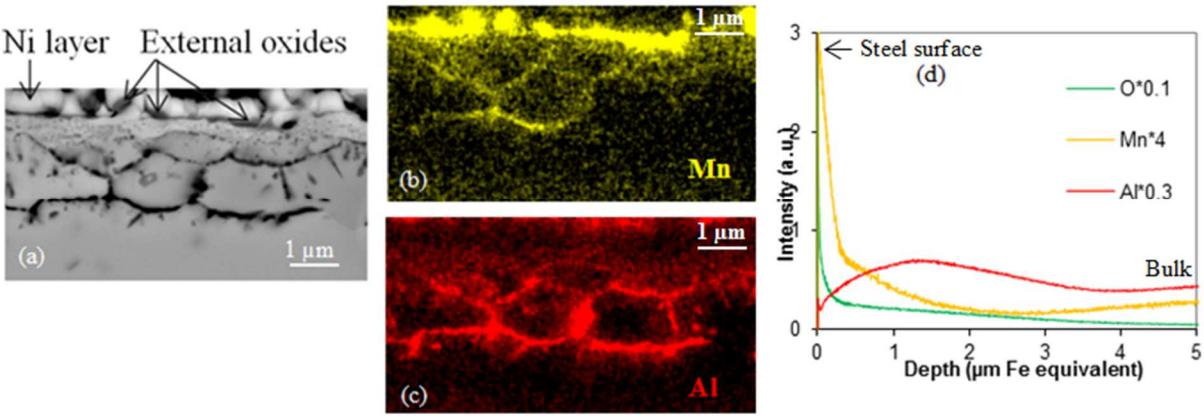

Figure 2: (a) SEM micrograph of the CSP specimen annealed in a gas atmosphere with *DP* = 0°C, (b) Qualitative elemental mapping of Mn, (c) Qualitative elemental mapping of Al, (d) GDOES spectra of O, Mn and Al

2. Inhibition layer

2.1. General features

SEM micrograph and EDX mappings (Figure 3) of the steel/coating interface after annealing in a gas atmosphere with *DP* = -40°C and galvanizing on CGL indicate that the inhibition layer is composed by a layer of Zn-rich compounds over a thin Al-rich layer. By considering the EDX mappings of Mn and O (Figures (d) and (e)), the external Al-Mn-O film described before (section 1) can be distinguished from the Al-rich phase of the inhibition layer (Figure 3 (c)). In addition, the latter seems to be discontinuous. It is worth to note that the external oxides are embedded in the inhibition layer.

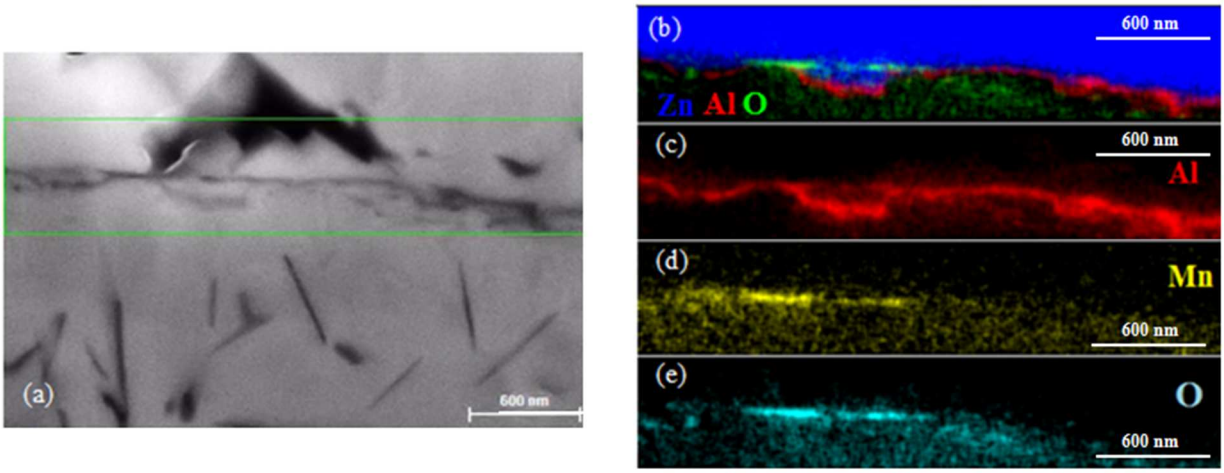

Figure 3: (a) SEM micrograph of CSP specimen annealed in a gas atmosphere with DP = -40°C and galvanized in a Zn bath with 0.122 wt.% Al, (b) EDX mapping of Zn-Al-O, (c) Al, (d) Mn and (e) O recorded from the selected area (green rectangle)

The general aspect of the inhibition layer on the sample annealed in a gas atmosphere with high *DP* (Figure 4) is akin to the one described above. The Al-rich layer present at the steel/coating interface in Figure 4 (c) corresponds to Fe-Al intermetallic compound since Al-rich oxides formed only underneath the steel surface in these annealing conditions. The MnO precipitates observed before galvanizing were incorporated to the inhibition layer (Figure 4 (d-e)). which appears discontinuous in some areas.

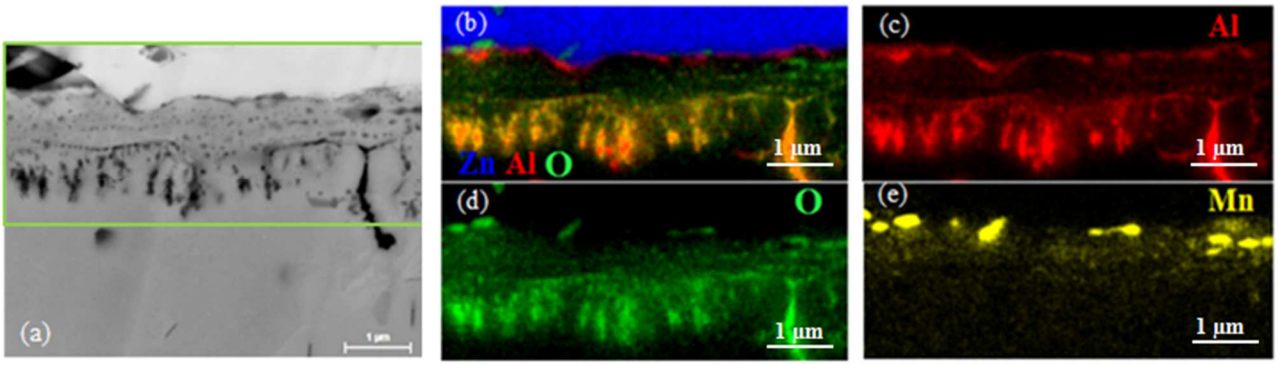

Figure 4: (a) SEM micrograph of CSP specimen annealed in a gas atmosphere with *DP* = -5°C and galvanized in a Zn bath with 0.122 wt.% Al, (b) EDX mapping of Zn –Al-O, (c) Al, (d) O and (e) Mn recorded from the selected area (green rectangle)

2.2. Phases determination

A discontinuous Al-rich layer has been observed on CSP specimens as shown in the previous section. However, EDX signal of Al in SEM could arise from Fe-Al intermetallic compounds, but also from Al external oxides, in particular for the sample annealed in a gas atmosphere with low *DP* = -40°C. Results from TEM characterization (Figure 5) on thin FIB foils allowed to quantitatively differentiate the Fe-Al intermetallic compound of the inhibition layer from Al oxides and to determine its chemical nature.

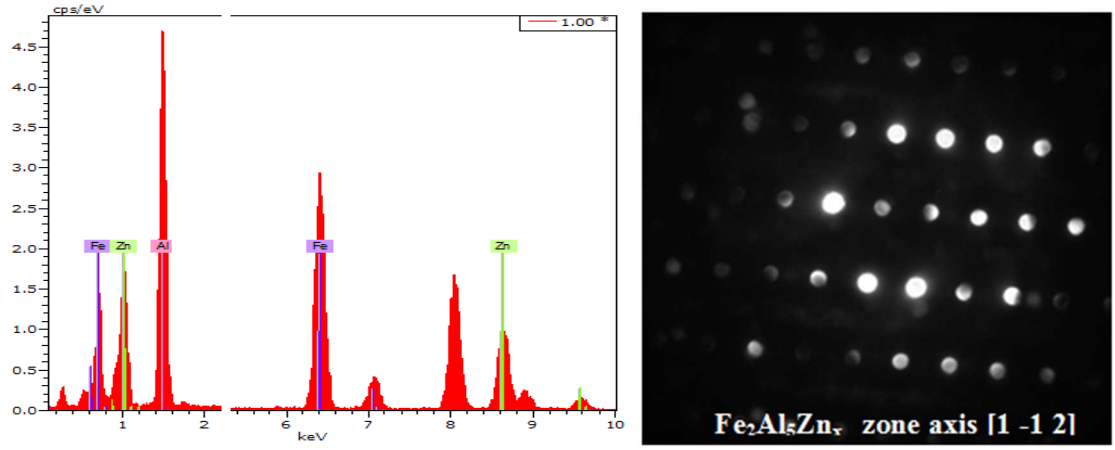

Figure 5: EDX spectrum (left) and Electron diffraction pattern (right) of Fe-Al intermetallic compound (right) of the inhibition layer formed on samples annealed in a gas atmosphere with low *DP* = -40°C

According to EDX (TEM) quantitative analysis (Table **2**), the Fe-Al intermetallic compound has a similar composition to $Fe_2Al_5Zn_x$ identified on IF substrates (38.5 wt.% Al, 36.9 wt.% Fe and 24.6 wt. % Zn [6]). Its structure is confirmed by the Electron Diffraction pattern shown in Figure 5 (right). JCPDS file #049-1381 (orthorhombic, space group Cmcm, lattice parameters a = 0.7656 nm, b = 0.6404 nm, c = 0.4241 nm) was used for indexing the experimental pattern.

Table 2: Chemical composition (wt. %) of intermetallic compounds present in the inhibition layer on the sample annealed in a gas atmosphere with *DP* = -40°C determined by EDX (TEM)

	$Fe_2Al_5Zn_x$	δ
Al	38.0 ± 1.4	1.8 ± 0.1
Fe	44.8 ± 1.3	10.0 ± 0.4
Zn	17.2 ± 0.6	88.2 ± 2.7

Concerning the Zn-rich phase, its chemical composition (Figure 6 (left) and Table 2) fits with the one reported by

Chen et al. [15] for δ phase (2.8 wt.% Al, 9.0 wt.% Fe and 88.2 wt.% Zn). The Electron Diffraction pattern taken from this phase (Figure **6** (right)) was indexed as δ phase by using the JCPDS file #45-1186 (hexagonal lattice, space group P, lattice parameters $a = b = 1.28$ nm, $c = 5.76$ nm). TEM results related to the galvanized sample after annealing in a gas atmosphere with *DP* = -5°C are not illustrated here, as they are definitely similar to the ones obtained for *DP* = -40°C.

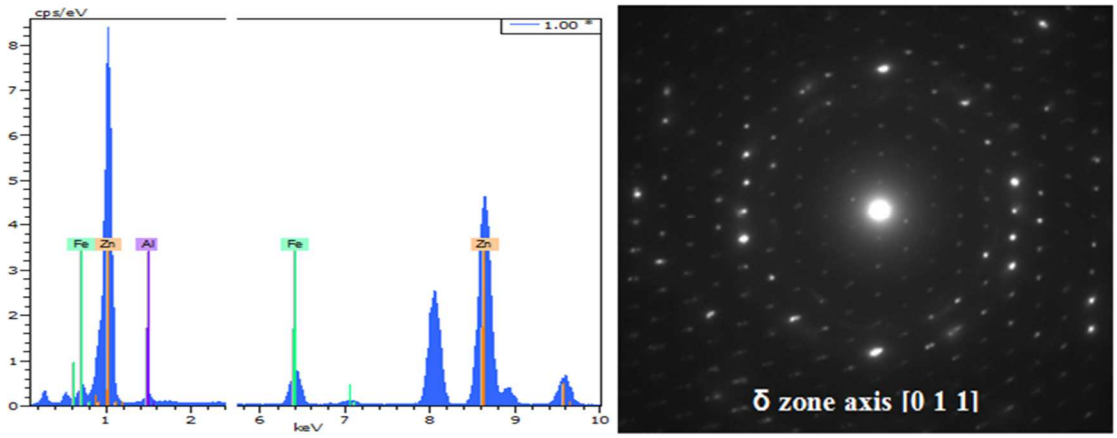

Figure 6: EDX spectrum (left) and Electron diffraction pattern (right) of Zn-rich phase (right) of the inhibition layer formed on sample annealed in a gas atmosphere with low *DP* = -40°C

Finally, TEM analyses revealed that the inhibition layer formed in a Zn bath with 0.122 wt.% Al on TRIP Mn-Al substrate is composed by discontinuous $Fe_2Al_5Zn_x$ and δ phase for both investigated recrystallization annealing conditions.

DISCUSSIONS

Despite the selective oxides on steel surface, reactive wetting by liquid Zn occurred and led to the formation of the inhibition layer. The mechanism for the formation of the inhibition layer in a GA bath in presence of external oxides can be summarized as follows: liquid Zn penetration into the porous / discontinuous film oxide (*DP* = -40°C) or in between nodular oxides (*DP* = -5°C) in order to reach the steel, Fe dissolution and supersaturation at the steel / liquid Zn interface, nucleation of $Fe_2Al_5Zn_x$ and/or δ phases. Subsequently, the inhibition layer incorporates the external oxides during its growth leading to the final structure illustrated in Figure 7. Similar interaction between liquid Zn, external oxides and substrate has been proposed by Sagl et al. [11] in the case of a Dual-Phase substrate galvanized in a GI bath (0.2 wt.% Al). It is worth to note that the inhibition layer in their study is composed essentially by $Fe_2Al_5Zn_x$ owing to the higher Al content in the Zn bath.

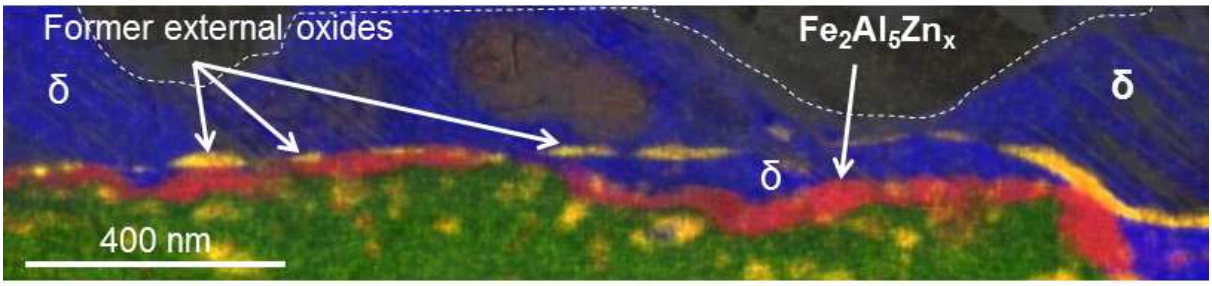

Figure 7: EDX (TEM) mapping on FIB foil prepared from a sample annealed in a gas atmosphere with *DP* = -40°C and galvanized in a Zn bath with 0.122 wt.% Al (Zn-blue, Al-red, Mn-yellow, Fe – green)

The observed microstructure of the inhibition layer can be explained through the diffusion path approach in the Al-Fe-Zn ternary phase diagram at 460°C [16,17] shown in Figure 8. This microstructure is comparable to one described by Zapico et al. on IF substrates [6]. Because of the discontinuity of $Fe_2Al_5Zn_x$ layer, two local microstructures are distinguished, namely $Fe/Fe_2Al_5Zn_x/δ/Zn$ and $Fe/δ/Zn$. Each sequence of phases can be described by real diffusion paths ① and ② as depicted in Figure 8. Moreover, the overall microstructure of the inhibition layer can be represented by the virtual diffusion path ③. Thus, a ternary equilibrium Fe - $Fe_2Al_5Zn_x$ - δ is established along the steel surface. The formation of δ phase enables all the interfaces to reach thermodynamic equilibrium. It can also be inferred that the

selective oxides at the steel surface do not affect the thermodynamic equilibrium.

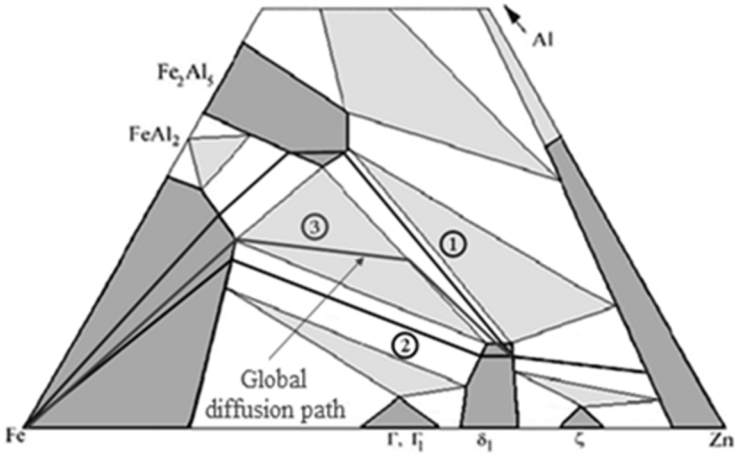

Figure 8: Diffusion paths on Zn-rich corner of Al-Fe-Zn ternary phase diagram at 460°C representing the local and the global microstructure of the inhibition layer investigated (adapted from [6])

CONCLUSION

The dew point (*DP)* of recrystallization annealing atmosphere modifies the morphology, the nature and the location of selective oxides with respect to the steel surface. Annealing in a gas atmosphere with low *DP* resulted in external Al-Mn-O film oxides, whereas high *DP* led to external MnO with a nodular shape. The selective oxidation state aforementioned allowed the reacting wetting by liquid Zn during hot-dipping in a typical GA bath. The resulted inhibition layer incorporated the external oxides during its growth.

The present study provides compelling evidence that the inhibition layer formed in a GA bath (0.122 wt.% Al) has a biphasic structure, namely a thick layer of δ upon a thin discontinuous layer of $Fe_2Al_5Zn_x$. We can point out that neither the recrystallization annealing atmosphere (*DP*) nor the steel substrate (TRIP, IF) affect the biphasic structure of the inhibition layer in the case of GA baths.

ACKNOWLEDGMENTS

The authors would like to thank Patrick Barges for TEM analysis. The authors also thank Sébastien Crémel for GDOES analysis and Annick Willems for the FIB thin foils preparation.

REFERENCES

1) M. Saito, Y. Uchida, T. Kittaka, Y. Hirose, and Y. Hisamatsu, “Formation Behavior of Alloy Layer in Initial Stages of Galvanizing,” *Tetsu--Hagane*, vol. 77, no. 7, pp. 947–954, 1991.

2) M. Guttmann, “Diffusive phase transformations in hot-dip galvanizing,” *Materials Science Forum, Vols. 155 - 156*, pp. 527–548, 1994.

3) L. Chen, R. Fourmentin, and J. R. M. Dermid, “Morphology and Kinetics of Interfacial Layer Formation during Continuous Hot-Dip Galvanizing and Galvannealing,” *Metall. Mater. Trans. A*, vol. 39, no. 9, p. 2128, Sep. 2008.

4) M. Úředníček and J. S. Kirkaldy, “Mechanism of iron attack inhibition arising from additions of aluminium to liquid Zn(Fe) during galvanizing at 450°C,” *Zeitschrift für Metallkunde 64*, pp. 899–910, 1973.

5) H. Yamaguchi and Y. Hisamatsu, “Reaction Mechanism of the Sheet Galvanizing,” pp. 649–658, 1979.

6) D. Z. Álvarez, F. Bertrand, J.-M. Mataigne, and M.-L. Giorgi, “Nature of the inhibition layer in GA baths,” *Metall. Res. Technol.*, vol. 111, no. 1, pp. 9–15, 2014.

7) N.-Y. Tang, “Determination of liquid-phase boundaries in Zn-Fe-Mx systems,” *J. Phase Equilibria*, vol. 21, no. 1, p. 70, Jan. 2000.

[8) E. M. Bellhouse and J. R. McDermid, “Selective Oxidation and Reactive Wetting during Galvanizing of a CMnAl TRIP-Assisted Steel,” *Metall. Mater. Trans. A*, vol. 42, no. 9, pp. 2753–2768, Sep. 2011.

9) K.-K. Wang, C.-W. Hsu, L. Chang, D. Gan, and K.-C. Yang, “Role of Al in Zn bath on the formation of the inhibition layer during hot-dip galvanizing for a 1.2Si–1.5Mn transformation-induced plasticity steel,” *Appl. Surf. Sci.*, vol. 285, Part B, pp. 458–468, Nov. 2013.

10) S. Prabhudev, S. Swaminathan, and M. Rohwerder, “Effect of oxides on the reaction kinetics during hot-dip galvanizing of high strength steels,” *Corros. Sci.*, vol. 53, no. 7, pp. 2413–2418, Jul. 2011.

11) R. Sagl, A. Jarosik, D. Stifter, and G. Angeli, “The role of surface oxides on annealed high-strength steels in hot-dip galvanizing,” *Corros. Sci.*, vol. 70, pp. 268–275, May 2013.

12) I. Aslam, B. Li, R. L. Martens, J. R. Goodwin, H. J. Rhee, and F. Goodwin, “Transmission electron microscopy characterization of the interfacial structure of a galvanized dual-phase steel,” *Mater. Charact.*, vol. 120, pp. 63–68, Oct. 2016.

13) X. S. Li, S.-I. Baek, C.-S. Oh, S.-J. Kim, and Y.-W. Kim, “Dew-point controlled oxidation of Fe–C–Mn–Al–Si–Cu transformation-induced plasticity-aided steels,” *Scr. Mater.*, vol. 59, no. 3, pp. 290–293, Aug. 2008.

14) J. Maki, J. Mahieu, B. C. D. Cooman, and S. Claessens, “Galvanisability of silicon free CMnAl TRIP steels,” *Mater. Sci. Technol.*, vol. 19, no. 1, pp. 125–131, Jan. 2003.

15) Z. W. Chen, J. T. Gregory, and R. M. Sharp, “Fe-Al-Zn ternary phase diagram at 450°C,” *Mater. Sci. Technol., Vol. 6, No. 12*, pp. 1173–1176, 1990.

16) Y. Leprêtre, J.-M. Mataigne, M. Guttmann, and J. Philibert, “Reactive interdiffusion in the Fe-Al- Zn system: Reaction mechanisms during hot-dip galvanizing,” *Zinc-Based Steel Coating Systems: Production and Performance (Edited by F.E. Goodwin), The Minerals, Metals & Materials Society*, pp. 95 – 106, 1998.

17) J.M. Mataigne, “Key mechanisms in galvanization of steel sheets,” *Rev Métall*, pp. 27–33, 2009.